Low-frequency acoustic wave generation in a resonant bubble layer

Oleg A. Druzhinin, Lev A. Ostrovsky, and Andrea Prosperetti

ARTICLES YOU MAY BE INTERESTED IN

Nonlinear wave interactions in bubble layers
The Journal of the Acoustical Society of America **113**, 1304 (2003); https://doi.org/10.1121/1.1539519

Linear pressure waves in bubbly liquids: Comparison between theory and experiments
The Journal of the Acoustical Society of America **85**, 732 (1989); https://doi.org/10.1121/1.397599

Effective medium approach to linear acoustics in bubbly liquids
The Journal of the Acoustical Society of America **111**, 168 (2002); https://doi.org/10.1121/1.1427356

Propagation of Sound Through a Liquid Containing Bubbles
The Journal of the Acoustical Society of America **19**, 481 (1947); https://doi.org/10.1121/1.1916508

Sound velocity and attenuation in bubbly gels measured by transmission experiments
The Journal of the Acoustical Society of America **123**, 1931 (2008); https://doi.org/10.1121/1.2875420

Nonlinear, low-frequency sound generation in a bubble layer: Theory and laboratory experiment
The Journal of the Acoustical Society of America **104**, 722 (1998); https://doi.org/10.1121/1.423308

Low-frequency acoustic wave generation in a resonant bubble layer

Oleg A. Druzhinin
Institute of Applied Physics, 603600 Nizhni Novgorod, Russia

Lev A. Ostrovsky
Institute of Applied Physics, and University of Colorado, CIRES/NOAA Environmental Technology Laboratory, Boulder, Colorado 80303

Andrea Prosperetti
Department of Mechanical Engineering, The Johns Hopkins University, Baltimore, Maryland 21218

The nonlinear response of a bubble layer subject to harmonic and biharmonic excitation at frequencies smaller than the individual bubble resonance frequency is considered. The nonlinear resonance properties of the layer and generation of difference-frequency signal are studied analytically and numerically. It is found that, for bubble volume fractions $\beta \approx 10^{-3}$ and pump amplitudes of the order of 10^{-1} atm, the power of the low-frequency signal (including waves radiated in both directions) may reach 10% of the total power of the incident biharmonic wave. The efficiency is restricted by the rapid formation of shocks already at relatively low driving amplitudes, which may not occur in a more complete model accounting for the inertia of the bubble pulsations. © *1996 Acoustical Society of America.*

INTRODUCTION

It is well known that bubbly liquids are characterized by acoustic nonlinearity that may become quite significant even at rather small bubble volume fractions.[1] Due to the large nonlinearity parameter, pressure waves in bubbly liquids cause various nonlinear phenomena even at comparatively small wave amplitudes. Many of the effects observed in other systems such as lasers, plasma, and electronic devices can therefore be expected to occur in such media.

In this paper we consider the effect of low-frequency sound generation through nonlinear interaction of two high-frequency waves analogous to conventional parametric arrays. The idea of using bubbles for enhancing the radiation of parametric arrays was discussed more than once (see, e.g., Refs. 2 to 4), but the realization of this effect encounters serious difficulties due to the prominent losses in bubbles. Nevertheless, a preliminary experiment with a bubble layer[3] has demonstrated this possibility with an observed signal pressure level several times larger than that in pure water. However, the effect was apparently far from being optimal due to the fact that losses grow in proportion to the nonlinearity of resonant bubbles, which played the key role in that case.

Here, we address another possibility, namely, the use of a layer of nonresonant bubbles (in which the losses are typically small, but nonlinearity is still sufficiently strong) together with the resonance properties of the layer as a whole. Even for a comparatively low volume fraction of bubbles, the sound speed c inside the layer can be considerably less than in pure water c_0. A simple estimate[1] shows that, e.g., at volume fraction of $\beta \approx 10^{-3}$, the ratio c_0/c of sound speeds in pure and bubbly liquids is close to 5. This causes strong reflections of the sound field from the layer boundaries and, hence, resonance effects. These resonance properties of the layer can be used to enhance the process of low-frequency signal generation when both the pumping waves and the difference-frequency wave (which in this case corresponds to the low-frequency output) are close to normal modes of the layer. In these conditions the effect is twofold. First, due to the prevalence of resonance conditions, the high-frequency beam is able to excite the layer more effectively. Second, due to the strong nonlinearity, the waves at two frequencies interact and produce a difference-frequency wave.

I. BASIC EQUATIONS

Let us consider a one-dimensional layer of bubbles of equal equilibrium radius R_0 and number concentration n_0 subject to an acoustic wave (Fig. 1). In the framework of the quasistatic model considered below, a generalization to the case of different size bubbles may be readily effected because only the total volume fraction of gas is involved in the theory.

The equation for the pressure field $P(x,t)$ in the bubbly mixture can be written in the form (see, e.g., Refs. 1, 5, and 6)

$$c_0^{-2} \frac{\partial^2 P}{\partial t^2} - \frac{\partial^2 P}{\partial x^2} = \rho_0 \frac{\partial^2 \beta}{\partial t^2}, \tag{1}$$

where c_0 and ρ_0 are the unperturbed sound speed and density of the liquid and the bubble volume fraction is denoted by $\beta(x,t)$.

In general, the Rayleigh equation for bubble oscillations should be used to close the formulation of the problem. However, in order to avoid the strong losses occurring near bubble resonance, it is advantageous to consider a situation in which the frequencies of interest are much smaller than
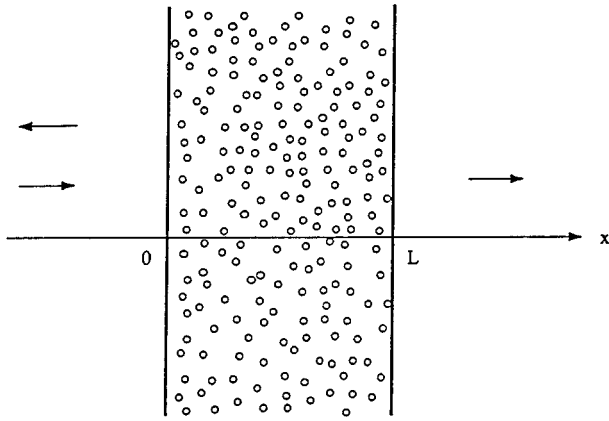
FIG. 1. Bubble layer under external pump.

the bubble resonance frequency approximately given by $\omega_b^2 = 3\gamma P_0/\rho_0 R_0^2$, where P_0 is the undisturbed pressure and γ the polytropic index. For these low frequencies, inertial effects associated with the bubble radial motion are small and a quasistatic dependence between the bubble radius (or volume) and the external pressure can be assumed,

$$\beta = \beta_0 (P/P_0)^{-1/\gamma}, \tag{2}$$

where the equilibrium volume fraction β_0 is given by

$$\beta_0 = \tfrac{4}{3}\pi n_0 R_0^3. \tag{3}$$

In what follows we shall assume an isothermal behavior so that $\gamma = 1$, which is compatible with the assumed relative slowness of variation of the pressure field. This approximation is valid under the condition $\omega \ll \kappa/R_0^2$, where κ is the thermal diffusivity of the gas within the bubble (see Ref. 1). The adiabatic case may be considered in a similar fashion with results that can be expected to be close to those presented here. The thickness of the layer l is assumed to be fixed so that β_0 is nonzero only for $0 < x < l$. In writing (2) we have also neglected surface tension effects.

It is convenient to introduce dimensionless variables defined by

$$x' = x/l, \quad t' = c_0 t/l, \quad \beta' = \beta/\beta_0, \quad P' = P/P_0. \tag{4}$$

Then, omitting primes, the equation for the pressure field can be rewritten as

$$\frac{\partial^2 P}{\partial t^2} - \frac{\partial^2 P}{\partial x^2} = A^2 \frac{\partial^2 P^{-1}}{\partial t^2}. \tag{5}$$

The parameter A, given by

$$A = \sqrt{\rho_0 \beta_0 c_0^2 / P_0}, \tag{6}$$

is of the order of the ratio of the speed of sound in the pure liquid to that in the bubbly liquid and is therefore generally large in the applications considered here. For example, with $P_0 = 10^5$ Pa, $c_0 = 1500$ m/s, $\rho_0 = 1000$ kg/m³, and $\beta_0 = 1.5 \times 10^{-3}$, $A^2 \simeq 30$.

For a plane layer subject to a normally incident plane wave, the conditions at the layer boundaries $x=0$ and $x=l$ correspond to the continuity of pressure P and particle velocity v, the latter being equivalent to the continuity of $\partial P/$

∂x under the approximation of Eq. (1). Indeed, it can be shown that nonlinear terms in the boundary conditions can be neglected for β much less than the characteristic nondimensional acoustic pressure amplitude p_{ac}/P_0 which, together with the condition $A^2 \gg 1$, gives the following limits for the range of bubble volume fractions to which the present model can be applied:

$$P_0/\rho c_0^2 \ll \beta_0 \ll p_{ac}/P_0.$$

Since the medium outside the layer is linear and nondispersive, we can assume

$$P_i = P_i(x - t), \tag{7}$$

for the incident wave and

$$P_r = P_r(x + t), \quad P_t = P_t(x - t), \tag{8}$$

for the reflected and transmitted waves.

Using the continuity conditions mentioned above, for $x=0$, we have

$$P_i(-t) + P_r(t) = P(0,t),$$
$$\frac{\partial P_i}{\partial x}(-t) + \frac{\partial P_r}{\partial x}(t) = \frac{\partial P}{\partial x}(0,t). \tag{9}$$

Upon differentiating the first equation with respect to time and using the relation $\partial P_r/\partial t = \partial P_r/\partial x$, we can eliminate the reflected wave to find

$$\frac{\partial P}{\partial t} - \frac{\partial P}{\partial x} = 2 \frac{\partial P_i}{\partial t} \quad \text{at } x=0. \tag{10}$$

Proceeding similarly, at $x=1$ we have

$$P(1,t) = P_t(1-t) \quad \frac{\partial P}{\partial x}(1,t) = \frac{\partial P_t}{\partial x}(1-t), \tag{11}$$

from which

$$\frac{\partial P}{\partial x} + \frac{\partial P}{\partial t} = 0 \quad \text{at } x=1. \tag{12}$$

Once P has been determined, the reflected and transmitted waves are readily found from the first of (9) and of (11), respectively.

In the analysis that follows we consider two cases. The first one corresponds to a weakly nonlinear regime when the amplitude of the harmonics generated by the nonlinearity is weak and standard perturbation methods can be applied. In the second case the pressure oscillations are strong enough to cause the formation of discontinuities (shocks). To deal with this situation, we represent the field inside the layer as the superposition of two oppositely propagating sawtooth waves.

II. WEAKLY NONLINEAR REGIME

We assume here that the pressure oscillations are small compared to the equilibrium value so that, upon setting

$$P = 1 + p, \tag{13}$$

$|p| \ll 1$. The equation for p is then readily found from (5) and is

$$(1+A^2) \frac{\partial^2 p}{\partial t^2} - \frac{\partial^2 p}{\partial x^2} = A^2 \frac{\partial^2}{\partial t^2} [p^2 - p^3 + O(p^4)]. \quad (14)$$

As mentioned before, we shall assume that $A^2 \gg 1$ and therefore we shall replace the factor $1 + A^2$ in the first term by A^2.

We first briefly discuss the linear resonance properties of the layer, when the right-hand side of (14) can be neglected.

A. Linear resonance properties of the layer

In the linear regime it is sufficient to consider a monochromatic incident wave given by

$$p_i = \tfrac{1}{2} p_{0i} \exp[i\omega(x-t)] + \text{c.c.}, \quad (15)$$

where c.c. denotes the complex conjugate term. In the steady state, the solution of the linear problem can be represented in the form

$$p = \tfrac{1}{2} p_+ \exp[i\omega(Ax-t)] + \tfrac{1}{2} p_- \exp[-i\omega(Ax+t)]$$
$$+ \text{c.c.} \quad (16)$$

The amplitudes $p_\pm$ readily follow from the boundary conditions (10) and (12):

$$\left(\frac{d}{dx} + i\omega \right) p = 2 p_{0i} \quad x = 0, \quad (17)$$

and

$$\left(\frac{d}{dx} - i\omega \right) p = 0 \quad x = 1. \quad (18)$$

From the second one we find

$$p_- = p_+ \xi \exp(2i\omega A), \quad (19)$$

with ξ the reflection coefficient:

$$\xi = \frac{A-1}{A+1} = 1 - \frac{2}{A} + O(A^{-2}). \quad (20)$$

It is readily verified that the substitution of $A^2 + 1$ by A^2 in (14) introduces an error of order $1/A^2$ in this expression. The other boundary condition (17) gives

$$p_+ = \frac{2(A+1)}{(A+1)^2 - (A-1)^2 \exp(2i\omega A)} p_{0i}. \quad (21)$$

The reflected and transmitted waves can be written as

$$p_t = \frac{p_{t0}}{2} \exp[i\omega(x-t)] + \text{c.c.}, \quad \text{for } x > 1, \quad (22)$$

and

$$p_r = \frac{p_{r0}}{2} \exp\{-i\omega(x+t)\} + \text{c.c.}, \quad \text{for } x < 0. \quad (23)$$

Upon substitution of the first one into the first of (11) we have

$$p_{t0} = [2A/(A+1)] p_+, \quad (24)$$

using which the amplitude p_{t0} is found from (21) to be

$$p_{t0} = \frac{4A}{(A+1)^2 - (A-1)^2 \exp(2i\omega A)} p_{0i}. \quad (25)$$

Similarly, the amplitude of the reflected wave follows from the first of (9):

$$p_{r0} = -\tfrac{1}{2}(A-1)[1 - \exp(2i\omega A)] p_+. \quad (26)$$

Equations (21) and (25) show that, for large A, a marked resonance occurs when the frequency of the incident wave is close to one of the eigenfrequencies of the layer given by

$$\omega_N = N\pi/A, \quad (27)$$

with N a positive integer. When ω equals any of these resonance frequencies, the reflected wave vanishes, while the amplitude of the transmitted wave is equal to that of the incident wave, $p_t = p_i$. Furthermore, from (21), in these conditions

$$p_+ = \tfrac{1}{2}(1 + 1/A) p_{0i}. \quad (28)$$

In the vicinity of the Nth resonance, i.e., for $|\omega - \omega_N| \ll \omega_N$, and for large A, we also find from (25) for the amplitude of the transmitted wave

$$|p_{t0}| \simeq \{[(\pi A/2\omega_1)(\omega - \omega_N)]^2 + 1\}^{-1/2} p_{i0}, \quad (29)$$

where $\omega_1 = \pi/A$ is the layer's first-mode frequency. According to this expression, the characteristic width b_r of the resonance curve is proportional to the factor ω_1/A or

$$b_r \simeq 2/A^2. \quad (30)$$

The physical origin of this damping is the radiation loss from the layer. Clearly, $b_r \to 0$ as $A \to \infty$ as expected.

B. Second harmonic generation

If the amplitude of the pressure oscillations is not very small, one should take into account nonlinear effects, namely, the generation of higher harmonics and the dependence of the resonance frequencies of the layer on the wave amplitude. We consider first the case of single-frequency excitation at some frequency ω. We limit ourselves to the most interesting case of near resonance in which ω is close to ω_N, one of the eigenfrequencies (27) of the layer.

Anticipating the presence of harmonic terms, we represent the corresponding pressure field in the layer as

$$p = p_1(x)\exp(-i\omega t) + p_2(x)\exp(-2i\omega t) + \cdots + \text{c.c.}, \quad (31)$$

where p_1 and p_2 are the spatial parts of the first and second harmonic, respectively.

The solution for the first harmonic can be represented in the form

$$p_1 \simeq \tfrac{1}{2} p_{01} \exp(-i\omega t)[\exp(iA\omega x) + \exp(-iA\omega x)] + \text{c.c.}, \quad (32)$$

where p_{01} is the amplitude, to be determined from the linear problem [cf. (21)]. In contrast to (16), we have assumed equal amplitudes of the two counterpropagating waves. This is justified by (19) in the limit of A large and ω close to one of the resonant modes. It may be noted that, in the third order of nonlinearity, the wave phase speed and wave number would depend on the amplitude, and therefore the nonlinear resonance may occur in the layer affecting the first-harmonic amplitude (see, e.g., Ref. 7). We have neglected this cubic

effect since in typical situations associated with bubbles the Q factor of the layer is not large enough to provide a considerable nonlinear shift of the resonance curve.

Upon substitution into (14), one finds that the field p_2 of the second harmonic is described by the equation

$$\frac{d^2 p_2}{dx^2} + 4A^2\omega^2 p_2 = 2A^2\omega^2 p_{01}^2 (1 + \cos 2A\omega x), \qquad (33)$$

with the boundary conditions

$$\left(\frac{d}{dx} \pm 2i\omega\right) p_2 = 0, \qquad (34)$$

at $x=0$ and $x=1$, respectively. In the present case where the pumping frequency is close to one of the linear eigenfrequencies (27) of the layer, i.e., $|\omega - \omega_N| \ll \omega_N$, to the leading order in A the solution for p_2 is

$$p_2 \simeq p_{02} \exp(-2i\omega t)\cos(2A\omega x) + \text{c.c.}, \qquad (35)$$

with the amplitude given by

$$p_{02} \simeq \frac{\pi A}{4}\frac{\omega}{\omega_1} p_{01}^2 \left[\left(\frac{\omega-\omega_N}{\omega_1}\pi A\right)^2 + 1\right]^{-1/2}. \qquad (36)$$

This relation shows that the second harmonic amplitude is affected both by the resonance at ω_N and at $2\omega_N$. Note that the former effect is typically stronger because p_{01}^2 contains the square of the resonant denominator [cf. (29)].

C. Low-frequency signal generation

Let us now turn to a pump wave consisting of two components at neighboring frequencies ω_N, ω_{N+1} corresponding to the Nth and $(N+1)$st linear layer eigenmodes

$$p_i = p_{0i}[\cos \omega_N(Ax-t) + \cos \omega_{N+1}(Ax-t)]. \qquad (37)$$

We wish to study the generation of a low-frequency field p_Ω at the difference frequency $\Omega = \omega_{N+1} - \omega_N$ under such conditions. In (37) we have taken the two components of the incident wave to have equal amplitude. One may expect the amplitude $|p_\Omega|$ to be small, as is usually the case for such problems.[1] Then, the equation for the low-frequency pressure field inside the layer is obtained from Eq. (14) in the form

$$\left(A^2\frac{\partial^2}{\partial t^2} - \frac{\partial^2}{\partial x^2}\right) p_\Omega = A^2\frac{\partial^2}{\partial t^2}(p^2)_\Omega, \qquad (38)$$

where $(p^2)_\Omega$ is the component of the forcing at the frequency Ω and, from (28), is given by

$$(p^2)_\Omega = \frac{1}{8}p_{0i}^2\left(1+\frac{1}{A}\right)^2 \exp(-i\Omega t)[\exp(i\Omega Ax)$$
$$+ \xi^2 \exp(-i\Omega Ax)] + \text{c.c.}, \qquad (39)$$

with the reflection coefficient ξ given by (20). At the layer boundaries $x=0$, $x=1$ the low-frequency component satisfies homogeneous boundary conditions:

$$\left(\frac{\partial}{\partial t} \mp \frac{\partial}{\partial x}\right) p_\Omega = 0. \qquad (40)$$

The solution of the problem (38), (40) can be represented as the sum of left- and right-propagating waves, each consisting of forced oscillations, and the lowest eigenmode of the layer

excited by the pumping. Thus the pressure field inside the layer is described by the expression

$$p_\Omega = (xp_+ + a)\exp[i\Omega(Ax-t)] + [(l-x)p_- + b]$$
$$\times \exp[-i\Omega(Ax+t)] + \text{c.c.} \qquad (41)$$

The amplitudes $p_\pm$ of the forced components are, from (38), (39),

$$p_+ = -\tfrac{1}{16}iA\Omega p_{0i}^2, \quad p_- = \xi^2 p_+. \qquad (42)$$

The amplitudes a, b of the layer eigenmode in the present case of resonance ($\Omega = \pi/A$), to the leading order in A, are derived from the boundary conditions in the form

$$a \simeq \tfrac{1}{4}A(p_+ + p_-) \simeq \tfrac{1}{2}Ap_+, \quad b \simeq a\xi \simeq a. \qquad (43)$$

The approximations in the last equality of both equations neglect terms of order $1/A$. With these results, the solution for the difference-frequency component of the pressure field inside the layer is given by

$$p_\Omega \simeq -ip_{0i}^2\frac{\pi}{16}\left\{\left[x + \frac{l}{4}A(1+\xi^2)\right]\exp\{i\Omega(Ax-t)\}\right.$$

$$+\left[\xi(l-x) + \frac{l}{4}A(1+\xi^2)\right]\xi \exp\{-i\Omega(Ax+t)\}\right\}$$

$$+ \text{c.c.} \qquad (44)$$

Recall that, for large A, $\xi \simeq 1$. It is clear from this expression that, in this resonant case, the largest contribution (of order A) to the low-frequency output comes from the layer eigenmodes excited by the pumping. From (11), (44), the following expression is derived for the amplitude of the low-frequency signal in the transmitted wave:

$$|p_\Omega^{\text{tr}}| \simeq \frac{\pi}{32}(1+\xi^2)(1+\xi)Ap_{0i}^2 \simeq \frac{\pi}{8}Ap_{0i}^2. \qquad (45)$$

It follows from this expression that the relative power of the low-frequency signal, which may be defined as the ratio $|p_\Omega^{\text{tr}}|^2/p_{0i}^2$, increases as the square of the incident wave amplitude and is proportional to A^2, i.e., it is the larger the smaller the losses caused by the radiation from the boundaries. Therefore, one can expect that the effect should be more pronounced for higher bubble concentrations.

III. SAWTOOTH WAVE THEORY

If the amplitude of the incident wave is large enough, one can expect the nonlinear distortions of the wave to lead to the formation of shocks. Clearly, the results discussed in the previous section are only valid when the incident wave amplitude p_{0i} is smaller than the threshold amplitude p_{0i}^{th} for shock formation. To estimate this quantity we proceed as follows.

Near the threshold, shock formation will occur only after multiple reflections from the layer boundaries. The situation is therefore similar to that of an initially sinusoidal plane wave propagating in an unbounded medium, a situation described by the well-known Bessel–Fubini solution. In this case the ratio of the second to the first harmonic just before

shock formation is given by $J_2(2)/2J_1(1)$. If we equate this ratio to p_{02}/p_+ given by (36) and (21), for resonance conditions $\omega=\omega_N$, we find

$$p_{0i}^{th} \simeq \frac{4J_2(2)}{J_1(1)\pi} \frac{1}{AN}. \tag{46}$$

This estimate shows that the threshold value decreases when A or the layer mode number N are increased. For example, for $N=9$ and $A^2=30$, we obtain

$$p_{0i}^{th} \simeq 0.02. \tag{47}$$

In the numerical experiments to be described presently, we find this estimate to be quite accurate. Consider then the case in which the incident wave amplitude considerably exceeds this threshold value, so that sawtooth waves are formed inside the layer. In this limit, the pressure field can be described in terms of sawtooth wave theory. In the case of a sufficiently large bubble concentration we can use an approach developed for nonlinear oscillations in resonators.[8,9] Suppose that the pressure field inside the layer can be approximated by a linear superposition of two sawtooth waves traveling in opposite directions:

$$p = p_+^s + p_-^s, \tag{48}$$

where

$$p_\pm^s = (p_{0\pm}^s/\pi)[\omega(\pm Ax-t) \mp 2\pi k], \tag{49}$$

with the value of the integer k chosen so as to reduce the quantity in brackets to a number comprised between $-\pi$ and π. Here $p_{0\pm}^s$ denote the amplitudes of the sawtooth waves. The sum (48) can be represented as a Fourier series as

$$p = \frac{1}{2i} \sum_m \{p_{+m}^s(x)\exp[i\omega_m(Ax-t)] + p_{-m}^s(1-x)$$

$$\times \exp[-i\omega_m(Ax+t)]\} + c.c., \tag{50}$$

where $\omega_m = m\omega \approx m\omega_N$. The dependence of the harmonic amplitudes on the spatial coordinate x is given by the known formula for the peak pressure of the sawtooth wave (see, e.g., Ref. 1)

$$p_{\pm m}^s(x) = \frac{p_{\pm 0m}^s}{1+2Nxp_{\pm 0}^s}, \tag{51}$$

where the amplitudes of the harmonics are related to the sawtooth wave amplitudes by

$$p_{\pm 0m}^s = (2/\pi m)p_{0\pm}^s. \tag{52}$$

In the steady state, the energy dissipated by the shocks and radiated from the boundaries is replenished by that of the pump wave via the first harmonic at the incident wave frequency ω. The amplitudes of the higher harmonics will be given in terms of $p_{\pm 01}^s$, the amplitude of the first harmonic, by (52). To calculate $p_{\pm 01}^s$ we use the boundary condition (10) to find, at $x=0$,

$$p_{+01}^s(A+1) - \frac{p_{-01}^s}{1+\pi N p_{-01}^s}(A-1) + \frac{i\pi N}{\omega}$$

$$\times \left[(p_{+01}^s)^2 - \left(\frac{p_{-01}^s}{1+\pi N p_{-01}^s} \right)^2 \right] = 2p_{0i}, \tag{53}$$

and, at $x=l=1$,

$$\frac{p_{+01}^s}{1+\pi N p_{+01}^s}(A-1)\exp(2i\omega lA) - p_{-01}^s(A+1)$$

$$- \frac{i\pi N}{\omega l} \left[(p_{-01}^s)^2 - \left(\frac{p_{+01}^s}{1+\pi N p_{+01}^s} \right)^2 \exp(2i\omega lA) \right] = 0. \tag{54}$$

For $|p_{\pm 01}^s| \ll 1$, the last terms in the left-hand sides of these equations (that arise from the derivatives $dp_\pm^s/dx$) can be omitted as they are of the second order in the amplitudes $p_{\pm 01}^s$. Then, from (54), one finds the following relation between the first-harmonic amplitudes of the left- and right-propagating waves:

$$p_{-01}^s = \frac{p_{+01}^s}{1+\pi N p_{+01}^s} \xi \exp(2i\omega lA), \tag{55}$$

where $\xi \approx 1$ for large A. The expression for the amplitude p_{+01}^s in the vicinity of the Nth linear resonance of the layer is then obtained from (53) and can be conveniently written in the form

$$p_{+01}^s \simeq \frac{[(1-p_{0i}\pi N)^2 + p_{0i}\pi N(A+1)]^{1/2}}{[(1-p_{0i}\pi N)^2 + p_{0i}\pi N(A+1)+(\Delta/\delta)^2\omega^2]^{1/2}} p_+^{res}, \tag{56}$$

where

$$\Delta = \frac{\omega-\omega_N}{\omega_1}, \quad |\Delta\omega| \ll 1, \tag{57}$$

and p_+^{res} is the value of the amplitude at exact resonance given by

$$p_+^{res} = (\pi N A)^{-1}\{[(1-p_{0i}\pi N)^2 + p_{0i}\pi N(A+1)]^{1/2}$$

$$- (1-p_{0i}\pi N)\}, \tag{58}$$

with

$$\delta^{-1} = \frac{\pi A}{2} \left(1 + 2\frac{p_{0i}\pi N-1}{A} \right). \tag{59}$$

Note that, for large A and $\pi N p_{0i}$ of the order unity, we have $\delta \approx 2/\pi A$, so that (58) reduces to

$$p_+^{res} \approx \sqrt{p_{0i}/\pi N A}. \tag{60}$$

Expressions for the first harmonic of the reflected and transmitted waves are directly obtained from the boundary conditions (9) and Eqs. (55), (56). Thus, in the vicinity of resonance, the following expressions are derived

$$|p_{tr}^{(1)}| \simeq (1+\xi) \frac{p_{+01}}{1+\pi N p_{+01}} \simeq \frac{2p_{+01}}{1+\pi N p_{+01}}, \tag{61}$$

$$|p_{\text{res}}^{(1)}| \simeq \frac{1}{2} p_{+01}(A-1) \frac{(1+\xi)\pi N p_{+01}}{1+\pi N(1+\xi)p_{+01}}$$

$$\simeq p_{+01} A \frac{\pi N p_{+01}}{1+2\pi N p_{+01}}. \tag{62}$$

When the incident amplitude is relatively small, and the attenuation of the shocks over the length of the layer is also small (i.e., $\pi N p_{+01} \ll 1$), from (61) it follows that $|p_{\text{tr}}^{(1)}| \approx 2 p_{+01}$, so that for large A we recover the result obtained earlier for shock waves in an acoustic resonator:[8]

$$p_{\text{tr}} \sim \sqrt{p_{0i}}. \tag{63}$$

In the other extreme case of large amplitudes, for which $\pi A p_{+01} \gg 1$ (but still with p_{+01} small compared to unity), shock attenuation is large. Then, from (61), (62) the following asymptotic expressions for the transmitted and reflected waves are obtained:

$$|p_{\text{tr}}^{(1)}| \simeq 2/\pi N, \tag{64}$$

$$|p_r^{(1)}| \simeq \tfrac{1}{2} A p_{+01}. \tag{65}$$

Equation (64) shows that in this case the system saturates in the sense that the amplitude of the transmitted wave does not depend upon that of the incident wave. This implies that shocks undergo strong losses with reflections at the right boundary $x=1$ nearly independent from those at the left boundary $x=0$.

IV. GENERATION OF LOW-FREQUENCY SIGNAL BY SAWTOOTH WAVES

Let us consider now the case of a biharmonic pump with frequencies equal to the resonances of the linear problem as in (37). In this case the pressure field inside the layer is described by an expression analogous to (50) with a slow modulation of the sawtooth wave. This modulation is caused by the modulation of the effective incident wave amplitude (37) that can be written as

$$p_i^e = 2p_{0i} \cos(\Omega/2)(Ax-t), \tag{66}$$

with $\Omega = \omega_{N+1} - \omega_N$ as before.

The characteristic time for attaining steady conditions in the layer can be defined as the damping time for free-mode oscillations due to shock losses. For sufficiently high amplitudes of the incident wave, this damping far exceeds the losses caused by radiation from the boundaries. Indeed, from Eqs. (51) and (52), for a given mode number N, we have the following estimate of the wave amplitude reduction after one passage through the layer:

$$\frac{p(1)}{p_{0i}} = \frac{1}{1+2p_{0i}N}.$$

Then, e.g., for the tenth mode, $N=10$ (considered in the numerical experiment), we find that the wave loses half or more of its initial amplitude due to shocks for incident wave amplitudes $p_{0i} > 0.05$ (typically used in the numerical calculations). Therefore, for waves of sufficiently large amplitude, the time of relaxation is of the order of the time for one passage through the layer and can be estimated as

$$\tau_{\text{rel}}^s \approx A. \tag{67}$$

Note that τ_{rel}^s is much less than the relaxation time calculated from the losses due to radiation from the boundaries, which, for $A \gg 1$, is given by [cf. Eq. (30)]

$$\tau_{\text{rel}}^b \simeq \frac{1}{b_r} \simeq \frac{1}{2} A^2.$$

Then, since the modulation time scale

$$\tau_{\text{mod}} \sim 4\pi/\Omega = 4A \tag{68}$$

exceed τ_{rel}^s one may consider the modulation slow enough that the solutions found above for the amplitude $p_\pm$ of steady sawtooth waves can be used in a quasisteady approximation allowing the parameter p_{0i} to depend on time.

The process of generation of the difference-frequency field is similar to that occurring in the weakly nonlinear case, but contributions to the low-frequency field now come from all the harmonics of the modulated sawtooth wave. Taking into account the relation (52) between the harmonic amplitudes and the fact that the damping affects all harmonics equally, we can add all the contributions. Thus, if the difference frequency field $p_\Omega^{(1)}$ due to the first harmonic of the sawtooth wave is known, the total value of the low-frequency field is simply given by

$$p_\Omega = p_\Omega^{(1)} \sum_{m=1}^{\infty} m^{-2} = \frac{\pi^2}{6} p_\Omega^{(1)}. \tag{69}$$

In order to estimate $p_\Omega^{(1)}$ we consider a problem analogous to Eqs. (38), (40) for the weakly nonlinear case, but with a different low frequency forcing term $(p^2)_\Omega^s$. This term is now obtained after averaging over the fast oscillations at the frequency $\frac{1}{2}(\omega_N + \omega_{N+1})$ and selecting the components of the forcing that are in resonance with the first layer mode, which is the one that provides the basic contribution to the low-frequency field generation.

Thus the expression for the driving field $(p^2)_\Omega^s$ is represented by the sum of two waves at the difference frequency Ω,

$$(p^2)_\Omega^s = p_{\Omega+} \exp[i\Omega(Ax-t)] + p_{\Omega-} \exp[i\Omega(Ax+t)] + \text{c.c.}, \tag{70}$$

with amplitudes $p_{\Omega\pm}$ given by

$$p_{\Omega+} = \frac{1}{4T} \int_0^1 dx \int_0^T dt \frac{p_{+1}^2(x,t)}{(1+\pi N p_{+1} x)^2} \exp[-i\Omega(Ax-t)], \tag{71}$$

$$p_{\Omega-} = \frac{1}{4T} \int_0^1 dx \int_0^T dt \frac{p_{-1}^2(x,t)}{[1+\pi N p_{-1}(1-x)]^2}$$

$$\times \exp[i\Omega(Ax+t)]. \tag{72}$$

The function p_{+1} corresponds to the resonance field in the layer and is given by (58) in which now the incident wave amplitude p_{0i} is taken to be variable as given in the right-hand side of (66). The other amplitude p_{-1} is given by an expression similar to (58) [see Eq. (77) below]. Written out in detail, the pertinent expressions are

$$p_{+1}(x,t) = \frac{1}{\pi NA}\{[(1-\pi Np_{0i}^{+}(x,t))^2 + A\,\pi Np_{0i}^{+}]^{1/2} - 1 + \pi Np_{0i}^{+}(x,t)\}, \tag{73}$$

$$p_{-1}(x,t) = \frac{1}{\pi A}\frac{[(1-\nu p_{0i}^{-}(x,t))^2 + A\,\pi p_{0i}^{-}]^{1/2} - 1 + \pi Np_{0i}^{-}(x,t)}{1 + A^{-1}\{[(1-\pi Np_{0i}^{-}(x,t))^2 + A\,\pi Np_{0i}^{-}]^{1/2} - 1 + \pi Np_{0i}^{-}(x,t)\}}, \tag{74}$$

where

$$p_{0i}^{\pm}(x,t) = 2p_{0i}\left|\cos\frac{\Omega}{2}(Ax\mp t)\right|. \tag{75}$$

For large A these expressions simplify to

$$p_{+1}(x,t) \simeq \sqrt{p_{0i}^{+}(x,t)/\pi NA}, \tag{76}$$

and

$$p_{-1}(x,t) \simeq \frac{[p_{0i}^{-}(x,t)/\pi NA]^{1/2}}{1 + [\pi Np_{0i}^{-}(x,t)/A]^{1/2}} \simeq \sqrt{\frac{p_{0i}^{-}(x,t)}{\pi NA}}. \tag{77}$$

As in the weakly nonlinear case, the pressure inside the layer can be represented as a superposition of forced oscillations and the layer eigenmodes excited by the pumping. Thus the pressure field is given by

$$p_{\Omega}^{s} = [p_{+}x + a]\exp[i\Omega(Ax - t)] + [p_{-}(1-x) + b]$$
$$\times \exp[-i\Omega(Ax + t)] + \text{c.c.}, \tag{78}$$

where the coefficients $p_{\pm}$ are defined by

$$p_{\pm} = -(i/2)A\Omega p_{\Omega\pm}, \tag{79}$$

and the coefficients a and b to the leading order in A are obtained from the boundary conditions in the form

$$a \simeq b \simeq -i(\pi A/8)(p_{\Omega+} + p_{\Omega-}). \tag{80}$$

Thus, for the transmitted wave amplitude, we have

$$|p_{\Omega}^{\mathrm{Tr}}| \simeq 4|a|. \tag{81}$$

Taking into account contributions from all the harmonics in the sawtooth waves we find the following expression for the difference-frequency signal:

$$|p_{\Omega}^{\mathrm{tr}}| = (\pi^3/12)A|p_{\Omega+} + p_{\Omega-}|, \tag{82}$$

where the amplitudes $p_{\Omega\pm}$ are given by (71), (72). The values of $p_{\Omega\pm}$ and the amplitude (81) of the low-frequency wave must be obtained numerically from (71), (72).

In an earlier paper,[10] the problem of the generation of a difference-frequency field under the influence of shocks was considered for the case of a traveling biharmonic wave with the help of some empirical solutions for the pressure. In the present case, however, the applicability of those result is not quite clear.

V. NUMERICAL RESULTS

Numerical integration of Eq. (5) with boundary conditions (10), (12) was performed by using an explicit scheme for $A^2 = 30$ so that the ratio of the sound speeds c_0/c_l equals $A \simeq 5.5$. The dimensionless width of the layer was set to be equal to $l = 10$ [this corresponds to a redefinition of the

length l in (4)]. Initially the pressure field inside the layer has the equilibrium value. After a time interval of the order $A/2$ a steady-state regime in the layer is usually reached [cf. estimate (67)].

In the simulations care was taken to select the time step h_t so as to capture the pressure variations in the shocks. Furthermore, the spatial step always satisfied the stability condition $h_t < Ah_x$.

The resonance curve for pumping at the first-mode frequency $\omega_1 = \pi/lA \simeq 0.056$ is well described by the linear theory result (25) for an incident wave amplitude $p_{0i} = 0.05$ (Fig. 2). Note that, according to the estimate (46) applied to the first mode, shocks should form for amplitudes $p_{0i} \gtrsim 0.18$.

At amplitudes p_{0i} exceeding the threshold for a frequency $\omega = 9\omega_1$, discontinuities of the pressure field form. The transient process, during which a steady-state sawtooth structure of the pressure field inside the layer is reached, consists of the formation of shocks and their summation after reflections from the layer boundaries. An example of such a transient process and the resulting steady-state pressure field inside the layer are shown in Fig. 3(a), (b), and (c).

In the comparison of numerical and analytical results a difficulty arises because the explicit numerical scheme used introduces numerical dispersion due to the discretization, so that high-frequency wave trains form (causing the shocks to oscillate) which were not taken into account in the analysis [in Fig. 3(b) these are related to the harmonics with
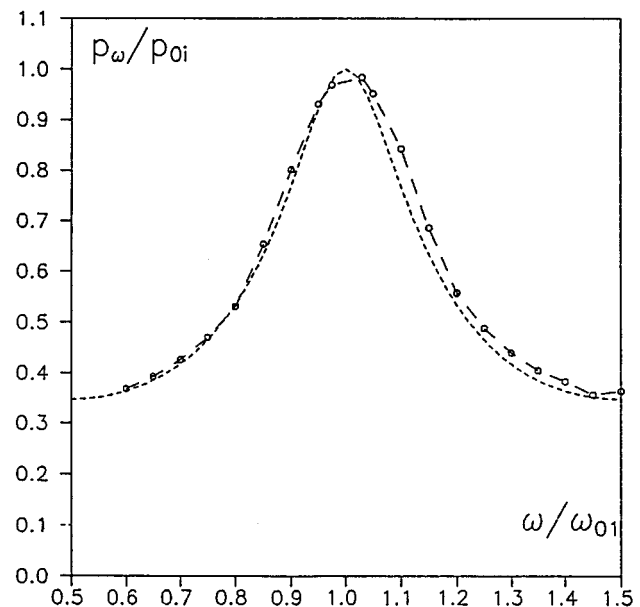

FIG. 2. Resonance curve of the first harmonic of the transmitted wave for $\omega_{0i} = \omega_1$, $p_{0i} = 0.05$; numerical data are marked by circles. The dotted curves correspond to the linear resonance (25).

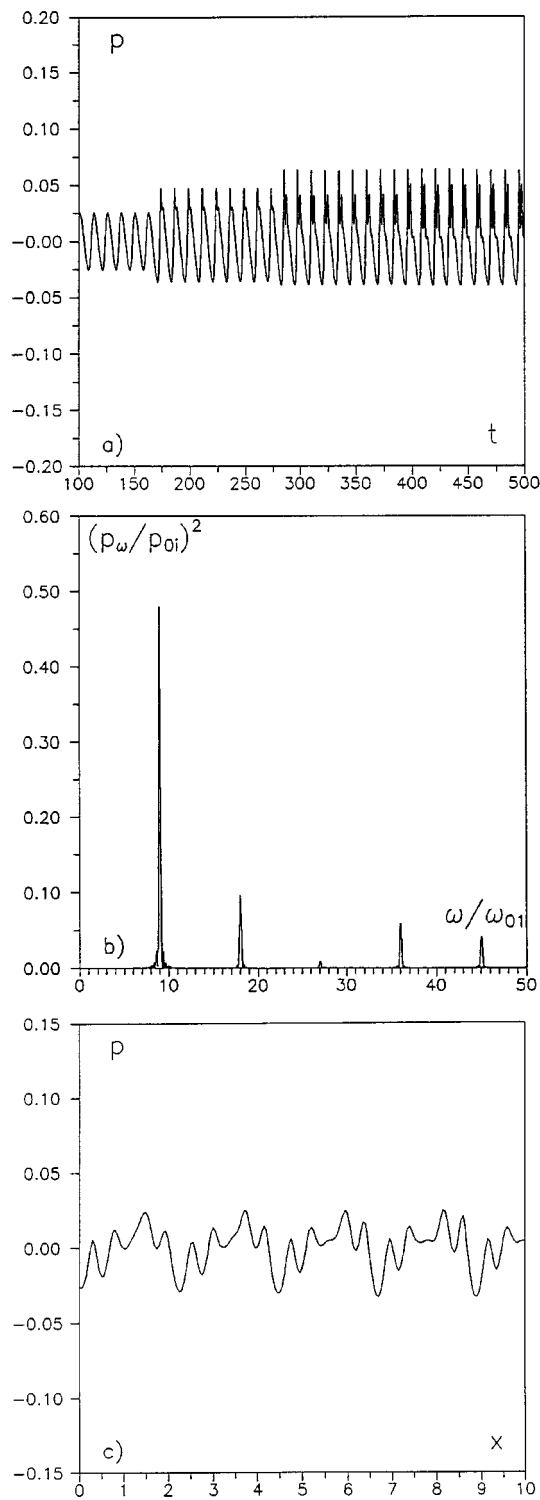Druzhinin *et al.*: Low-frequency wave generation in bubble layers

FIG. 3. (a) Pressure oscillations in the transmitted wave for $p_{0i}=0.05$, $\omega=9\omega_1$. (b) Relative power spectrum of the transmitted wave (i.e., power spectrum normalized by factor p_{0i}^2) for $p_{0i}=0.05$, $\omega_{0i}=9\omega_1$, $600<t<1000$. (c) Pressure field inside the layer at $t=500$ for $p_{0i}=0.05$, $\omega_{0i}=9\omega_1$.

FIG. 4. (a) First harmonic amplitudes of the transmitted and reflected waves normalized by p_{0i}. Numerical results for transmitted and reflected waves are marked by stars and crosses, respectively. Long- and short-dashed curves correspond to solution (61) and (62) for the transmitted and reflected wave amplitudes. (b) Resonance curves of first harmonics of the transmitted wave. Circles and squares correspond to the numerical results obtained for $p_{0i}=0.05$ and $p_{0i}=0.1$, respectively. The dotted curve corresponds to the linear resonance curve (29), the solid line represents the sawtooth wave resonance (62) for $p_{0i}=0.05$.

$\omega_n/\omega_1>27$]. On the other hand, a similar dispersion can be caused by bubbles, if a correction to the quasistatic model is taken into account (below we discuss this point in more detail). In this case the effect of shocks is not quite equivalent to that of viscous losses, which are usually implied for sawtooth waves (see, e.g., Ref. 1). Comparison of the numerica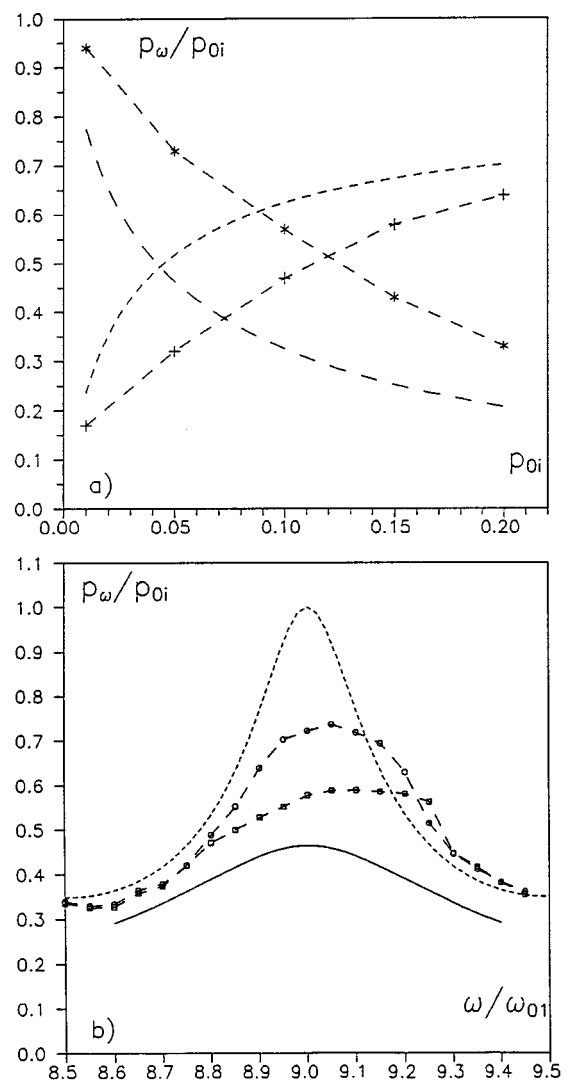l results for transmitted and reflected waves with those provided by the sawtooth wave theory [Fig. 4(a)] shows some differences that may be related to the effect mentioned above. However, in the case of comparatively small amplitudes of the incident wave, the analytical results given by Eqs. (58) and (61), (62) [obtained for the case of weak shock losses, dashed and short-dashed curves in Fig. 4(a), respectively] quite accurately describe the numerical data for transmitted and reflected waves.

Figure 4(b) shows the resonance curves obtained for the transmitted wave first harmonic $\omega/\omega_1=9$. Note that losses related to shocks significantly affect the resonance so that, for an amplitude $p_{0i}=0.1$ [marked by the empty squares in Fig. 4(b)], the resonance structure of the layer in correspondence of the higher modes is blurred by the losses.

In order to study the low-frequency signal output, we consider pumping at two neighboring frequencies $\omega^{(1,2)}$ cor-
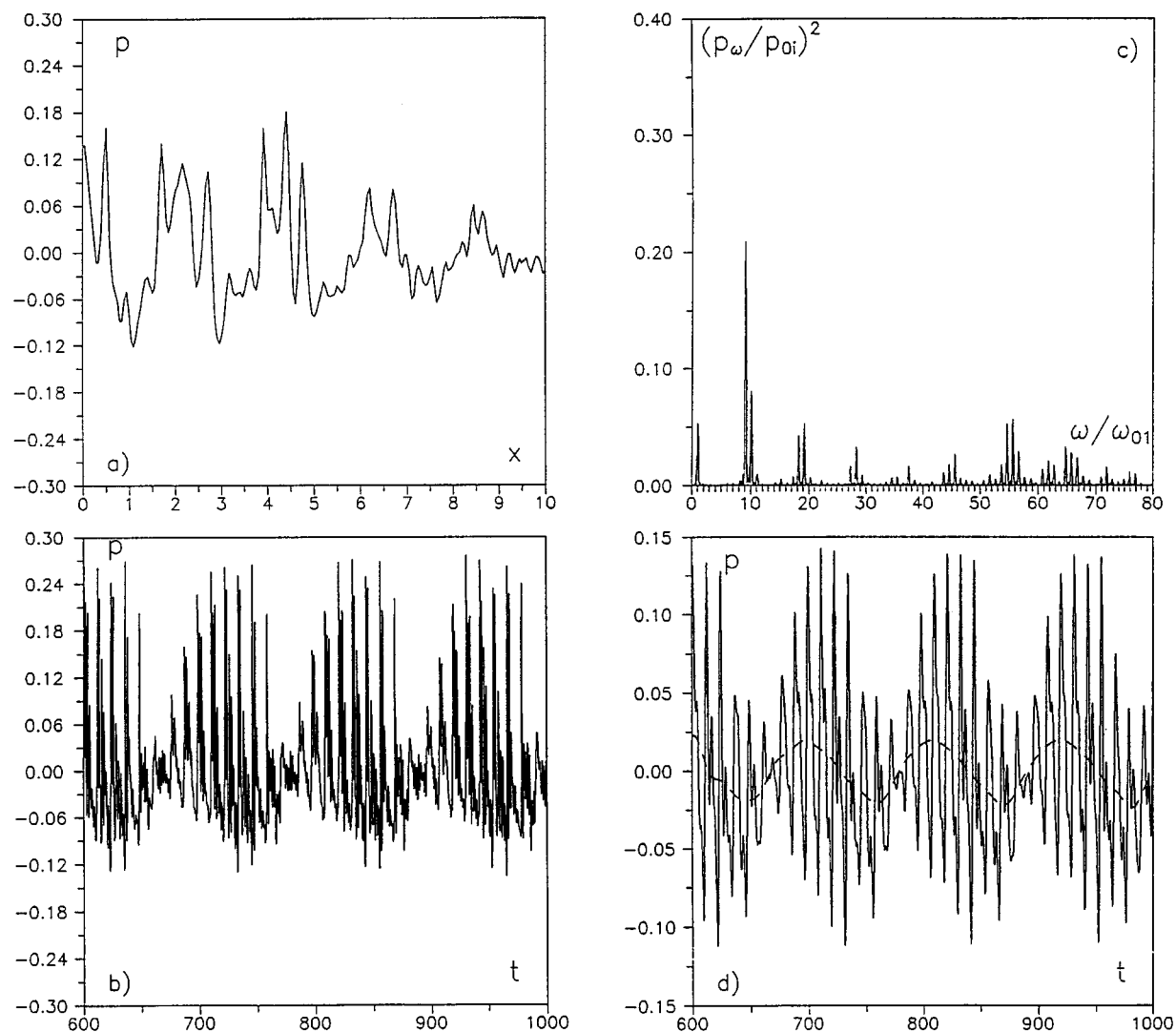
FIG. 5. (a) Pressure field inside the layer at $t=1000$ for biharmonic pumping at frequencies $\omega^{(1)}=9.1\omega_1$, $\omega^{(2)}=10.1\omega_1$ with amplitudes $p_{0i1}=p_{0i2}=0.1$. (b) Pressure oscillations in the transmitted wave of Fig. 4(a). (c) Power spectrum of the transmitted wave derived from time series represented in (b). (d) Pressure oscillations in the transmitted wave obtained after filtering (solid line). The dashed line shows the low-frequency signal.

responding to the 9th and 10th modes of the layer.

The pressure field inside the layer calculated for an amplitude $p_{0i}=0.1$ is presented in Fig. 5(a). Pressure oscillations at the right boundary of the layer and the corresponding power spectrum are are shown in Fig. 5(b) and (c). We used filtering to eliminate the high-frequency oscillations related to shocks (for frequencies $\omega>30\omega_1$). The result presented in Fig. 5(d) corresponds to the superposition of sawtooth waves (full curve). The dashed curve corresponds to the difference-frequency harmonic.

We also calculated the maximum of the relative power of the low-frequency signal in the transmitted wave. This value is defined as the maximum of the square of the ratio of difference-frequency harmonics to the the incident power $(p_\Omega^{tr}/p_{0i})^2$. To find this maximum we calculated the low-frequency output within a range $8.5<\omega^{(1)}/\omega_1<9.5$ of incident harmonics frequencies, changing the frequency of both waves and keeping the difference frequency fixed and equal to the layer first mode frequency, $\Omega=\omega^{(2)}-\omega^{(1)}=\omega_1$. The dependence of the low-frequency output on the incident

wave amplitude is shown in Fig. 6(a). In the case of sufficiently small amplitudes ($p_{0i}<0.05$), both the weakly nonlinear theory given by Eq. (45) and the sawtooth theory results provided by Eq. (81) with harmonic amplitudes given in Eqs. (73), (74) [corresponding to the dotted and dashed curves in Fig. 6(a), respectively] agree well with the numerical data (empty circles). However, for larger amplitudes, the numerical results differ from those predicted by the sawtooth theory. This difference can be explained by the effect of the high-frequency oscillations on shocks discussed above. Correspondingly, the contribution of the harmonics to the low-frequency signal output is larger than that predicted by sawtooth theory.

The dependence of the low-frequency output on the frequency ω of one pumping wave (the frequency of the other wave being the sum of ω and the first mode resonance frequency $\omega_1=\Omega$) is presented in Fig. 6(b). Note that, as the parameter p_{0i} is increased, the resonance properties of the layer become less pronounced with respect to high modes, while the resonance for the first mode is still intact.
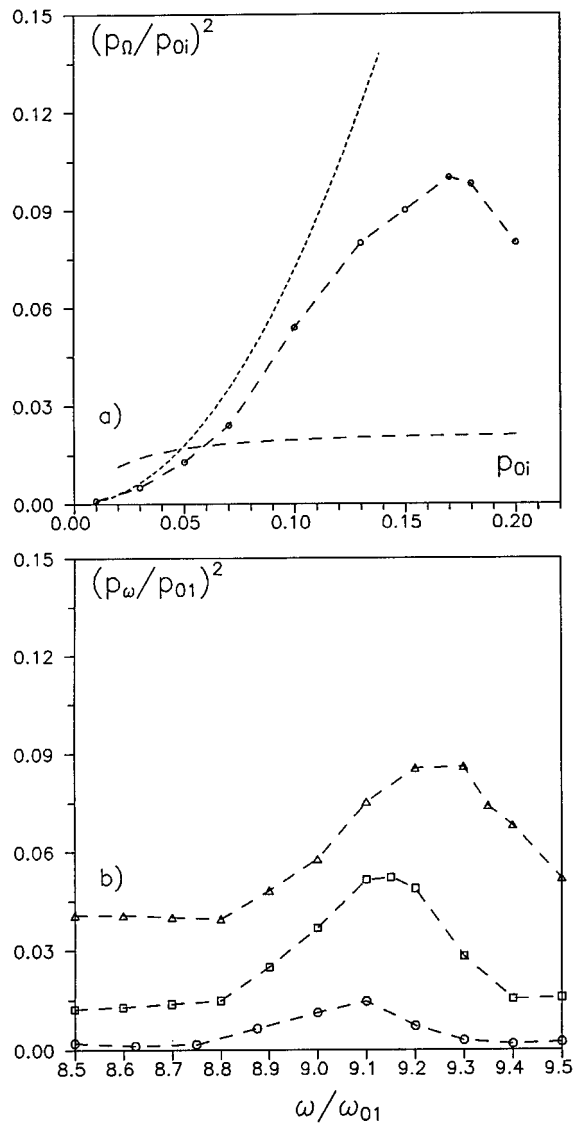
FIG. 6. (a) Dependence of the maximum of the relative power of the low-frequency output on the incident wave amplitude p_{0i} for biharmonic pumping at frequencies $\omega^{(1)}, \omega^{(2)} = \omega^{(1)} + \omega_1$ in the range $8.5\omega_1 < \omega^{(1)} < 9.5\omega_1$. The circles are the numerical results. The dotted and dashed curves show the weakly nonlinear and sawtooth theory results (45) and (81), respectively. (b) Dependence of the relative low-frequency output on $\omega^{(1)}$ (with frequency $\omega^{(2)} = \omega^{(1)} + \omega_1$) for amplitudes $p_{0i} = 0.05$ (circles), 0.1 (squares), and 0.15 (triangles).

VI. DISCUSSION

The nonlinear response of a bubble layer subject to an external pumping at a frequency much smaller than the bubble resonance frequency has been studied. The approximate quasistatic solution of the Rayleigh equation for the bubble radius and linearized boundary conditions for the pressure field have been used. The bubble concentration has been taken to be sufficient for both the nonlinear and resonance properties of the layer to be significant. In particular, low-frequency signal generation by a high-frequency biharmonic pumping has been studied analytically and numerically in the case when the frequencies of both incident waves and the low-frequency wave correspond to the layer eigenmodes.

The results obtained show that in the case of resonance

the efficiency of the low-frequency signal generation can become as large as 10% of the incident power for bubble concentrations of the order $\beta \approx 10^{-3}$ (see Fig. 6). Such an efficiency can be considered large in comparison with the typical ones of parametric arrays for which, due to the high losses, the low-frequency output usually does not exceed 10^{-3}.

The results presented in this paper are affected by shock formation inherent to our quasistatic (nondispersive) model. Numerical dispersion, which becomes significant when nonlinear distortion of the wave front takes place, introduces some dispersion analogous to the one that would be caused by bubbles. Upon accounting for the correction to the quasistatic solution due to the inertia of the oscillating bubbles, the expression (2) for the bubble volume fraction is given by[1]

$$\beta \approx \beta_0 \left[\frac{P_0}{P} - \frac{1}{\omega_b^2} \frac{\ddot{P}}{P_0} \right],$$

where ω_b is the bubble resonance frequency. This correction results in an additional term in the equation (5) for the pressure

$$A^2 D \frac{\partial^4 p}{\partial t^4},$$

where

$$D = \frac{A^2 \rho_0 c_0^2}{3 \gamma P_0} \frac{R_0}{l},$$

where R_0 and l are the bubble radius and layer width, respectively.

Numerical dispersion results in a similar correction but with a factor $D_{\text{num}} \approx h_t^2/12$, where h_t is the dimensionless time step. Thus for $A^2 = 30$, $h_t \sim 10^{-2}$, and the parameters c_0, ρ_0 typical of pure water at atmospheric pressure $P_0 \sim 10^5$ Pa, we obtain for the ratio of the "equivalent" bubble radius to the layer width the following estimate

$$R_{\text{eq}}/l \sim 10^{-4}. \tag{83}$$

Therefore, the numerical dispersion affecting the present calculations is equivalent to the dispersion that would be introduced by bubbles with a radius of this order of magnitude. For instance, for $l \approx 0.2$ m, the equivalent bubble radius would be of the order of 20 μm.

[1] K. A. Naugol'nykh and L. A. Ostrovsky, *Nonlinear Wave Processes in Acoustics* (Nauka, Moscow, 1990, in Russian), translation published by Cambridge U.P.

[2] E. A. Zabolotskaya and S. I. Soluyan, "Emission of harmonics and com-

bination frequency waves by air bubbles,'' Sov. Phys. Acoust. **18**, 396–398 (1973).

[3] L. M. Kustov, V. E. Nazarov, L. A. Ostrovsky, A. M. Sutin, and S. V. Zamolin, ''Parametric acoustic radiation with a bubble layer,'' Acoust. Lett. **6**, 15–17 (1982).

[4] L. M. Kustov, V. E. Nazarov, and A. M. Sutin, ''Wave front reversal for an acoustic wave in a bubble layer,'' Akust. Zh. **31**(4), 837–839 (1985), (in Russian).

[5] R. E. Caflisch, M. J. Miksis, G. C. Papanicolaou, and L. Ting, ''Effective equation for wave propagation in bubbly liquids,'' J. Fluid Mech. **153**, 259–273 (1985).

[6] K. W. Commander and A. Prosperetti, ''Linear pressure waves in bubbly liquids: comparison between theory and experiments,'' J. Acoust. Soc. Am. **85**, 732–746 (1989).

[7] J. Kevorkian and J. D. Cole, *Perturbation Methods in Applied Mathematics* (Springer-Verlag, New York, 1981), Sec. 4.4.

[8] L. A. Ostrovsky, ''On shock waves in acoustical resonators,'' Akust. Zh. **20**(1), 140–142 (1974) (in Russian).

[9] V. V. Kaner, O. V. Rudenko, and R. V. Khokhlov, ''On the theory of nonlinear oscillations in acoustical resonators,'' Akust. Zh. **23**(5), 756–765 (1977) (in Russian).

[10] A. M. Sutin, ''On the limiting regime in ultrasonic parametric array,'' Akust. Zh. **24**(1), 104–107 (1978) (in Russian).